Journal of Visualization, Vol. 3, No. 2 (2000) 125-133

Performance Evaluation of an Optical Flow Technique Applied to Particle Image Velocimetry Using the VSJ Standard Images

Quénot, G. M.*

* CLIPS-IMAG, B.P. 53, 38041 Grenoble Cedex 9, France.

Received 7 January 2000.
Revised 13 April 2000.

***Abstract*:** A Dynamic Programming based Optical Flow technique has been applied to the Particle Image Velocimetry (PIV) problem. It has been used for the extraction of dense velocity fields in a planar section of a fluid flow illuminated by a thin laser light sheet. Two (in-plane) components of the velocity vectors can be recovered using a single camera and all three components can be recovered using two or three cameras. Quantitative performance tests have been carried out on calibrated synthetic image sequences from the PIV Standard Project of the Visualization Society of Japan (VSJ). Results are presented for the 2D flow based sequences (STD01 to STD08 Standard Images) and the 3D flow based sequences (STD301, STD302, STD331 and STD337 Standard Images). The RMS error is within the 2-3% range and within the 4-8% range for recovery of the two-component and the three-component velocity vectors respectively.

Keywords: particle image velocimetry, optical flow, dynamic programming, VSJ Standard Images, performance evaluation.

1. Introduction

The experimental fluid mechanics technique of Particle Image Velocimetry (PIV) has proven to be a valuable method for quantitative two-dimensional flow structure evaluation (Hesselink, 1988). It enables the measurement of the instantaneous in-plane velocity vector field within a planar section of the fluid flow. Using two or more cameras, the measurement of the out-of-plane velocity component is also possible. Nowadays, almost all PIV is done by computer image processing on digital images (DPIV, Willert and Gharib, 1991) and most methods are based on image intercorrelation.

One of the main drawbacks of classical DPIV is its inability to accurately resolve flow regions characterized by large velocity gradients. This is due to the strong deformation of the particle image pattern within a DPIV search window. Hence, several alternative evaluation methods have been proposed to remove this limitation (Huang et al., 1993; Tokumaru and Dimotakis, 1995; Merzkirch and Gui, 1996).

It has been shown (Quénot et al., 1998) that an Optical Flow method is also an interesting alternative, offering high accuracy without most of the typical DPIV limitations. This motion estimation technique, known as Orthogonal Dynamic Programming (ODP, Quénot, 1992 and 1996), is in some sense similar to the Image Correlation Velocimetry proposed by Tokumaru and Dimotakis (1995).

The objective of the present study is to better characterize the performance of the ODP optical flow technique for PIV using publicly available synthetic image sequences (Standard Images) from the PIV Standard Project of the Visualization Society of Japan (Okamoto et al., 1997). Three velocity measurement problems were considered for this evaluation:

- Recovery of the two velocity components in a two-dimensional flow,
- Recovery of the two in-plane velocity components in a three-dimensional flow,
- Recovery of the three velocity components in a three-dimensional flow.

Dense vector fields are recovered in a planar section of the fluid flow illuminated by a thin laser light sheet and compared with the known correct vector fields.

2. Optical Flow for Particle Image Velocimetry

Optical flow computation consists in extracting a dense velocity field from an image sequence assuming that the intensity (or color) is conserved during the displacement. Many techniques have been developed for the computation of optical flow. Not all of these are well suited for the DPIV problem. Many require long image sequences that are not easily obtainable experimentally and/or do not perform very well on the particle image texture (especially multi-resolution methods).

The technique that was chosen for the PIV application was introduced as the Orthogonal Dynamic Programming (ODP) algorithm for optical flow detection from a pair of images (Quénot, 1992). The originality of this algorithm is that it transforms the (complex) search problem for two-dimensional alignments into a carefully selected sequence of (simple) search problems for monodimensional alignments. It is based on an iterative search for a continuous and regular velocity field that brings the second image over the first one while minimizing the L_1 or L_2 (Minkowski) distance between them. The technique has been extended to be able to operate on longer sequences of images and to search for subpixel displacements (Quénot, 1996). The ODP based PIV will be referred to as ODP-PIV. It cannot be detailed here but it is fully explained in Quénot et al. (1998); it can be related to classical intercorrelation techniques but with the following differences:

- Basic matching is searched on elastic image strips (either horizontal or vertical) instead of being searched on rigid blocks, and robust strip matching is performed using Dynamic Programming which enforces continuity and regularity constraints,
- A global, dense, continuous and coherent image matching is iteratively updated and refined using alternatively horizontal and vertical strip matchings and by reducing the strips' width and spacing along with the iterations,
- The technique is able to operate on multiband (e.g. color) images,
- It can be applied simultaneously to sequences of more than two images,
- It can search for subpixel displacements,
- It provides dense vector fields (1 velocity vector for every pixel, neither holes nor border offsets).

3. The PIV-STD Project of the Visualization Society of Japan

The PIV-STD research group of the Visualization Society of Japan (VSJ) has developed standard image sequences (called "Standard Images") for performance evaluation and comparison of PIV systems (Okamoto et al., 1997). They are distributed via Internet (http://www.vsj.or.jp/piv/) or by CDROM and publicly available. Standard Image test sequences are proposed for 2D and 3D flows. A Custom Made Standard Image generator program is also available (in the 2D case only) to generate image sequences with user-defined characteristics.

The VSJ PIV Standard Images have already been used for the evaluation of the cross correlation method (Hu et al., 1998). However the Standard Images were not originally designed for quantitative evaluation and comparison of PIV systems but rather for the development, test and qualitative evaluation of PIV systems. Therefore, synthetic image sequences with the correct corresponding flow field were provided but nothing about a quantitative evaluation protocol, like a vector field comparison program or a way to display the results, was included. However, it was found later that it would be useful too and could quite easily be achieved. An addition has been made to the VSJ corpus providing such an evaluation protocol usable in the same way by any organization (Quénot and Okamoto, 2000). This protocol is also publicly available via Internet (http://clips.imag.fr/mrim/georges.quenot/vsj-eval/evaluation.html). It includes programs (with C source code) to perform the quantitative performance measure and a standard way to display the results in order to permit easy system performance comparison. There are actually three distinct protocols, dedicated respectively to the evaluation of PIV systems on the three different types of PIV problems previously mentionned and addressed through three different types of Standard Images sequences so that evaluations can be carried out independently on any of them.

The ODP-PIV system was evaluated using this protocol and results are presented here with Standard Image sequences based on 2D flows (STD01to STD08 and Custom-Made Standard Images), and 3D flows both for the recovery of the two in-plane components (STD301 and STD302) and of all three components (STD331 and STD337) of the velocity vectors (always in a planar section of the fluid flow).

4. Recovery of the Two Velocity Components in a 2D Flow

The first standard image sequence (STD01) is a "typical" case defined by the following parameters: N = 4000 (number of particles), T = 33 ms (time interval, defining the scale of the in-plane velocity), v = 7.39 pixel/interval (in-plane velocity), L = 20.0 mm (light sheet thickness, defining the scale of the out-of-plane velocity), w = 0.017 -/interval (out-of-plane velocity, fraction of the particles leaving and entering the light sheet per interval), P_a = 5.0 pixel (average particle diameter) and P_d = 1.4 pixel (standard deviation of particle diameter). The seven following standard image sequence (STD02 to STD08) differ from the typical case by only one parameter. The images are 256 × 256 pixels representing an actual 100 mm × 100 mm area. The ratio between the average in-plane and out-of-plane velocities is of about 0.12 (defining a 2D flow). Figure 1 shows one image of the first sequence, four consecutive superimposed images and the used velocity field. The shape of the particles in these sequence is gaussian and the diameter is associated with e^{-1} times the central value (in contrast with the e^{-2} used conventionally by many authors).

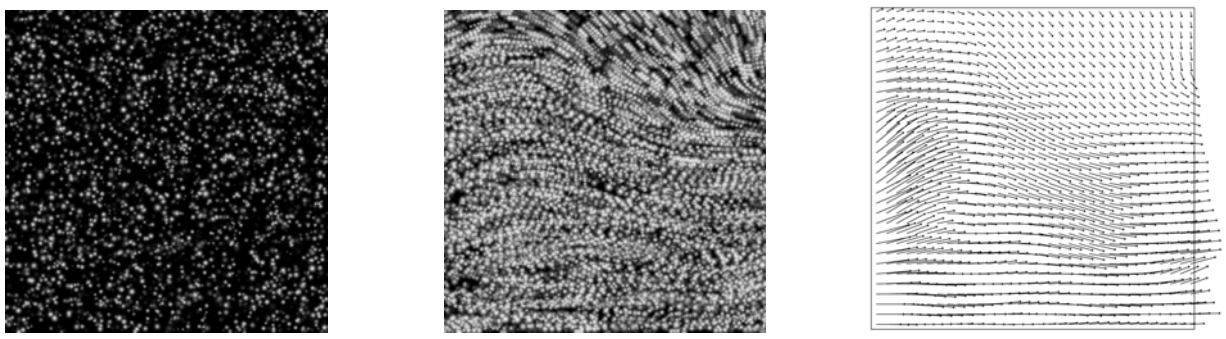

Fig. 1. One particle image, four superimposed images and the correct velocity field.

Table 1 displays the parameter sets used for the eight standard sequences as well as the absolute (in pixels/s) and relative (in percentage) RMS error for the ODP-PIV method using respectively two, three and four consecutive images. ODP-PIV control parameters are tuned differently for low and high out-of-plane velocity (only for STD08). The ODP-PIV method always provide a velocity vector for each pixel in the image (of course, the actual spatial resolution of the vector field may be quite lower depending upon the particle size and density) but the correct vector fields are given only for locations subsampled 8 times in both directions (i.e. on a 32 × 32 grid) and the RMS error is computed using only these 1024 locations.

Table 1. RMS error on the STD01 to STD08 VSJ standard sequences.

No.	N	T	v	L	w	Pa	Pd	2 images	3 images	4 images
STD01	4000	33	7.39	20.0	0.017	5.0	1.4	10.2 (4.20%)	9.59 (3.94%)	9.33 (3.83%)
STD02	4000	**100**	22.4	20.0	0.058	5.0	1.4	35.6 (14.6%)	32.3 (13.2%)	32.8 (13.4%)
STD03	4000	**10**	2.24	20.0	0.006	5.0	1.4	24.8 (10.2%)	24.5 (10.0%)	24.4 (10.0%)
STD04	**10000**	33	7.39	20.0	0.017	5.0	1.4	7.44 (3.05%)	5.21 (2.14%)	4.54 (1.86%)
STD05	**1000**	33	7.39	20.0	0.017	5.0	1.4	11.0 (4.52%)	9.23 (3.79%)	8.47 (3.48%)
STD06	4000	33	7.39	20.0	0.017	5.0	**0.0**	10.5 (4.34%)	4.86 (2.00%)	4.33 (1.78%)
STD07	4000	33	7.39	20.0	0.017	**10.0**	4.0	12.0 (4.94%)	8.27 (3.40%)	7.98 (3.28%)
STD08	4000	33	7.39	**2.0**	0.170	5.0	1.4	33.9 (13.9%)	15.2 (6.26%)	12.2 (5.02%)

Particles that are included in the count may have a quite low peak intensity according to their distance from the center of the light sheet and many are hardly visible. Also, at high particle counts (STD04) or at large particle diameters (STD07) significant particle overlap may occur. These two characteristics are not a problem for the ODP-PIV method since it tracks the image texture rather than individual particle. The more irregular the texture is and the wider the spatial frequency of the resulting image is, the less ambiguous it is also when global coherency constraints are enforced by the method.

The typical case parameters appear to be non-optimal for the ODP-PIV method for the particle density (at least 2.5 times too small) and size (twice too big). However, the default in-plane velocity scale is near the optimum and the out-of-plane velocity has negligible effect (except for the STD08 sequence).

The RMS error for the typical case (STD01) is about 4% using two, three or four images. Severe accuracy degradation occurs when the average in-plane velocity is far (3 times smaller or larger, STD02 and STD03) from the optimum one. Increasing the particle density (STD04) highly improves the accuracy while decreasing again the particle density (STD05) does not further degrade the accuracy. Reducing the particle diameter standard deviation improves the accuracy (STD06) as well as increasing the particle diameter (STD07, however this is linked to the insufficient particle density). Finally, high out-of-plane velocity (STD08, 17% of particle appearance and disappearance per interval) significantly degrades the accuracy. However, even in this case, an accuracy of about 5% is obtained using the four images. Near the optimal particle density (STD04), the accuracy is as good as 3% using only two images and below 2% using the four images.

Custom image sequences were also generated using the version 2 of the CustomMade Standard Image generator program in order to evaluate the effect of the various tunable parameters and to search for the optimal image parameters for the system. By running several tests with various parameter configurations (Quénot, 1999), it was found that for the ODP-PIV system:

- The optimal number of particles for the method is above 10000 (one particle by 6.4 square pixels density), which is the maximum allowed by the sequence generation program. However, it is estimated from the data that the optimal density without that limitation would be about the same.
- The optimal particle diameter is around 2.5-3.0 pixel. Combined with a high particle density (implying many particle overlap), this seems to provide the wider spatial frequency distribution for the tracked texture. With an even lower particle size, a sampling problem probably arises.
- The optimal average in-plane velocity is of about 6-8 pixel/interval. This last value may change for higher relative out-of-plane velocities (*w*, a value of 0.05, about three times higher than that of the typical Standard Images, was used here).

5. Recovery of the Two In-plane Velocity Components in a 3D Flow

The recovery of the two in-plane components of 3D flows is almost the same problem as the recovery of 2D flows. The third (out-of-plane) component, however, is no longer supposed to be negligible; it is not recovered but makes the problem more difficult by inducing much higher rates of particle appearance and disappearance.

STD301 contains a single 145-image continuous sequence (of a jet impinging on a wall at 12 cm/s with a Reynolds number of 3000, with a time step of 5 ms) as well as the correct vector field for each time step. The target flow field is a 4 cm × 4 cm × 2 cm volume and the laser light sheet thickness is 2 mm (with a gaussian profile). The average number of particles in images (256 × 256) is 4000 and the average particle diameter is of 5 pixels with a standard deviation of 2 pixels. STD302 is identical to STD301 except that the average number of particles in images is 1000 instead of 4000. The minimum, average and maximum values of the *w* parameter (specifying the average percentage of particles entering and leaving the light sheet at each time step) are respectively of 3.67%, 6.08% and 8.52% (to be compared to 1.70% for the standard typical "2D" case).

Vector fields have been recovered from the image sequences for all possible time steps using from 2 to 7 consecutive images and compared to the corresponding known correct one. Again, the correct vector fields are given only for locations subsampled 8 times in both directions (on a 32 × 32 grid) and the RMS error is computed only on these 1024 locations. The RMS errors have been computed for every possible time step in the sequences and the global RMS values have then been computed for both sequences. Table 2 displays the absolute (in pixel/interval) and relative (in percentage) global RMS errors. Using more than two consecutive images significantly improve the accuracy.

Table 2. RMS error on the STD301 and STD302 VSJ test sequences.

	STD301 4000 particles	STD302 1000 particles
2 images	0.260 (5.10%)	0.352 (6.88%)
3 images	0.193 (3.78%)	0.294 (5.75%)
4 images	0.159 (3.10%)	0.258 (5.05%)
5 images	0.141 (2.75%)	0.246 (4.81%)
6 images	0.137 (2.69%)	0.234 (4.58%)
7 images	0.147 (2.87%)	0.245 (4.79%)

Figure 2 shows plots of the RMS errors according to the timestep and the number of consecutive images used. It also shows a plot of the evolution of the global characteristics of the flow field according to the timestep and a plot of Table 2.

It may be noticed that the parameters chosen for the virtual PIV experimental setup here are not the optimal ones for the ODP-PIV method as it has been mentioned in the previous section. STD301, which is much closer to the optimal conditions than STD302, produces much better results for the recovery of the same flow field. Even better results could probably be obtained using more smaller particles but the possibility to generate custom sequences with tuning of these parameters like in the 2D case does not currently exist for the 3D sequences.

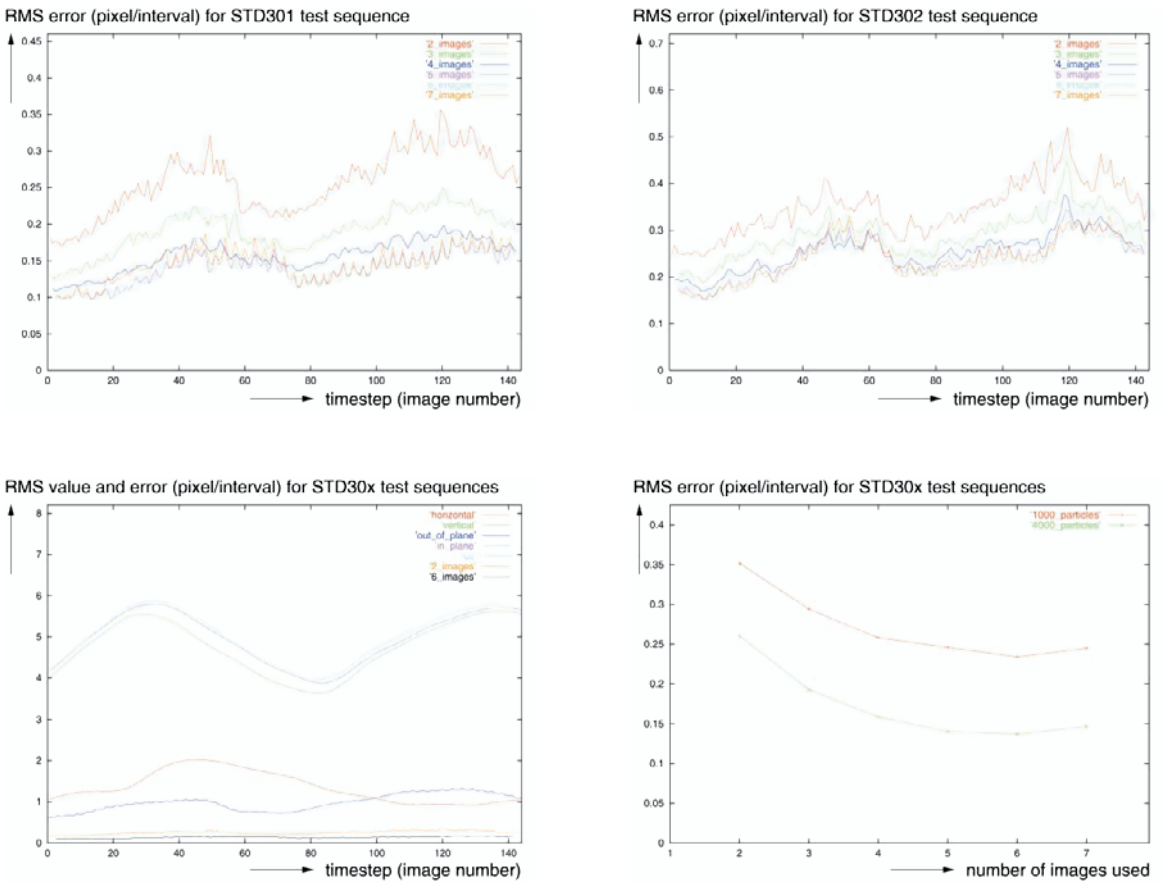

Fig. 2. Top: plot of the RMS error with timestep using from two to seven consecutive images for the STD301 (left) and STD302 (right) test sequences; bottom left: plot of the per component (horizontal, vertical, out-of-plane, in-plane, and full vector) RMS values of the correct vector field (common to the STD301 and STD302 test sequences) with RMS error using repectively two and six consecutive images of the STD301 test sequence; bottom right: plot of the global RMS error with the number of consecutive images used for the recovery of the vector fields at the 1000 (STD302) and 4000 (STD301) particle density.

6. Recovery of the Three Velocity Components in a 3D Flow

Stereo PIV is used to recover also the third (out-of-plane) component of the velocity vectors. Figure 3 shows the stereo PIV virtual experimental setup used with STD331 and STD337 Standard Images. Images are taken simultaneaously from three different cameras, all three being 6 cm far from the center of the visualized flow field: camera 1 is centered and cameras 0 and 2 are respectively 30 degrees off on the left and on the right. The target flow field is a 4 cm × 4 cm × 2 cm volume and the visualized flow field is a 1.2 cm × 1.2 cm × 0.2 cm volume (with a gaussian laser light sheet profile) for STD331 and a 2 cm × 2 cm × 0.2 cm volume for STD337. Also, the flow field is assumed to be in water (n = 1.33) while cameras are in air (n = 1.00), both being separated by a wall at 3 cm from the visualized flow field. The average number of visible particles in images (256 × 256 pixels) is 4000 for STD331 and 6800 for STD337, and the average particle diameter is of 5 pixels with a standard deviation of 2 pixels.

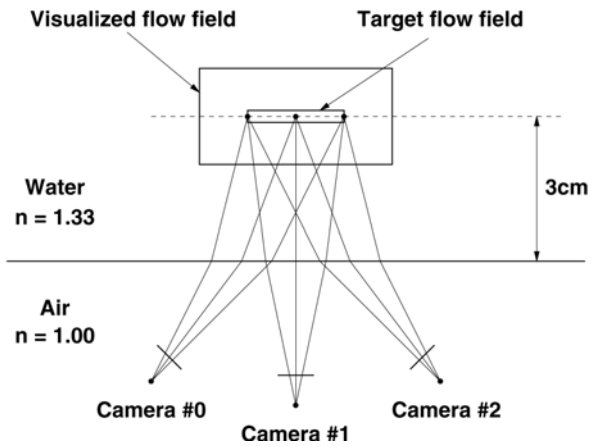

Fig. 3. Stereo PIV virtual experimental setup (top view).

STD331 contains three 145-image continuous sequences (of a jet-impinging on a wall at 15 cm/s with Reynolds number of 3000, the timestep is 5 ms) taken by the three cameras (Fig. 3). STD337 differs from STD331 by: the sequences are 201-image long each, the time step is 2 ms, and the average number of visible particles in images and the visualized flow field are different as mentioned in the previous paragraph. The exact 3D vector field to be recovered is also provided for comparison (Fig. 4). It is provided for 9×9 locations for STD331 and for 41×41 locations for STD337. Only the subset of the 81 or 1681 corresponding locations that are visible from the three viewpoints simultaneously are used for the computation of the RMS error.

Compared to the two-component case, the computation process has three steps here:

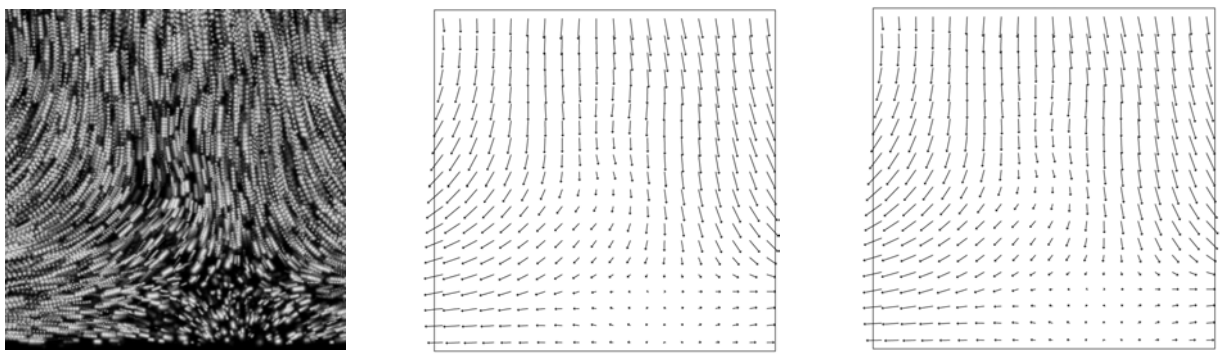

Fig. 4. Vector fields from the VSJ sequence 337, from left to right: 7 superimposed images from center camera, correct vector field (in-plane component), recovered vector field (in-plane component; though not displayed here, the out-of-plane component is also recovered).

- Computation of the apparent 2D vector field for each camera independently,
- Alignment of these 2D vector fields on the planar search area,
- Building the three-component vector from two or three two-component vectors.

The first step is identical to the classical two-component search (using from 2 to 7 consecutive images) and is done separately for each camera. The two following steps consist in simple geometric transformations that make use of the camera calibrations (the exact camera model is used here, the camera calibration problem is not considered). The last step makes use of a least square method.

Like in the case of STD301 and STD302, a vector field has been computed for every timestep and compared to the corresponding known correct vector field. An RMS error has been computed on all three velocity components for every timestep and a global RMS error on the whole sequence has been computed. Table 3 displays the global absolute RMS error (in cm/s) according to the number of images used (3×2 to 3×7) as well as the global characteristic parameters of the sequence.

Table 3. Absolute RMS error (in cm/s) on the STD331 and STD337 VSJ test sequences, *v* is in pixel/interval and *w* is in -/interval, (*) STD331 with manual filtering of erroneous vector fields.

No.	*N*	*T*	*v*	*L*	*w*	P_a	P_d	3×2	3×3	3×4	3×5	3×6	3×7
STD331(*)	4000	5	10.0	2.0	0.077	5.0	2.0	0.624	0.532	0.434	0.366	0.339	0.363
STD337	6800	2	2.64	1.0	0.076	5.0	2.0	1.203	1.014	0.950	0.823	0.799	0.776

A few severely erroneous vector fields were obtained for STD331. This illustrates one weakness of the ODP method which is somehow a drawback of its strength: since a global match between images is searched for with continuity constraints enforced by the use of dynamic programming, either ambiguities are correctly resolved using neighborhood information (general case) or local errors are propagated globally and lead to a completely wrong vector field (when approaching the limits of operation). However, such completely wrong vector field can easily be detected by a simple visual inspection. Results in Table 3 are presented after removing them. This can be seen as a failure of the ODP-PIV on STD331 (on from 1 to 6% of it) and is due to the fact that, again, the characteristic image parameters are far from the optimal conditions: a too high in-plane velocity (10.0 pixels/interval) is combined with a too low particle density (4000). On the other hand, STD337 also has non-optimal characteristic parameters with a too low in-plane velocity (2.64 pixels/interval); this does not prevent a good matching but it greatly reduces the accuracy of the result (since there is a lower limit on the absolute error in pixel/interval, its effect becomes more important). With characteristic parameters closer to the optimal values, significantly better results could probably be achieved for the recovery of the same flow fields (no erroneous vector fields for STD331 and much better accuracy for STD337).

Table 4. Per component RMS error on the STD331 VSJ test sequence, with manual filtering of erroneous vector fields: density is 137/144 (95%) with 2 images, 135/143 (94%) with 3 images, 137/142 (96%) with 4 images, 137/141 (97%) with 5 images, 135/140 (96%) with 6 images and 138/139 (99%) with 7 images.

	Horizontal	Vertical	Out-of-plane	In-plane	**Full**
STD331	3.989 (42.4%)	7.929 (84.4%)	3.058 (32.5%)	8.876 (94.5%)	**9.388 (100%)**
3×2 images	0.207 (2.20%)	0.282 (3.00%)	0.516 (5.49%)	0.350 (3.73%)	**0.624 (6.64%)**
3×3 images	0.190 (2.02%)	0.253 (2.69%)	0.428 (4.55%)	0.317 (3.37%)	**0.532 (5.66%)**
3×4 images	0.157 (1.67%)	0.219 (2.32%)	0.341 (3.62%)	0.269 (2.86%)	**0.434 (4.62%)**
3×5 images	0.134 (1.43%)	0.197 (2.09%)	0.277 (2.95%)	0.238 (2.53%)	**0.366 (3.89%)**
3×6 images	0.126 (1.33%)	0.180 (1.92%)	0.258 (2.74%)	0.220 (2.34%)	**0.339 (3.60%)**
3×7 images	0.128 (1.35%)	0.183 (1.94%)	0.287 (3.05%)	0.223 (2.37%)	**0.363 (3.86%)**

Tables 4 and 5 show more detailed results: the absolute (in cm/s) and relative (in percentage) RMS error for each velocity component. Table 5 also shows the results obtained using only two cameras separated either by 60 or 30 degrees. Removing the center camera induces no significant loss in accuracy while, as expected, using a narrow angle induces a significant loss, especially for the out-of-plane component. Again also, using more than two consecutive images significantly improve the accuracy.

Table 5. Per component RMS error on the STD337 VSJ test sequence using images from all three cameras, from two cameras separated by a 60-degree angle and from two cameras separated by a 30-degree angle.

	Horizontal	Vertical	Out-of-plane	In-plane	**Full**
STD337	5.163 (50.1%)	8.058 (78.2%)	3.807 (36.9%)	9.570 (92.9%)	**10.30 (100%)**
3 × 2 images	0.390 (3.78%)	0.580 (5.62%)	0.979 (9.50%)	0.699 (6.78%)	**1.203 (11.6%)**
3 × 3 images	0.321 (3.11%)	0.552 (5.35%)	0.788 (7.65%)	0.638 (6.19%)	**1.014 (9.84%)**
3 × 5 images	0.266 (2.58%)	0.464 (4.50%)	0.625 (6.07%)	0.535 (5.19%)	**0.823 (7.99%)**
3 × 7 images	0.257 (2.49%)	0.428 (4.15%)	0.594 (5.76%)	0.499 (4.84%)	**0.776 (7.53%)**
2 × 2 images	0.430 (4.17%)	0.600 (5.82%)	0.979 (9.50%)	0.739 (7.17%)	**1.226 (11.9%)**
2 × 3 images	0.346 (3.36%)	0.563 (5.47%)	0.788 (7.65%)	0.661 (6.42%)	**1.029 (9.99%)**
2 × 5 images	0.280 (2.72%)	0.464 (4.50%)	0.625 (6.07%)	0.542 (5.26%)	**0.828 (8.03%)**
2 × 7 images	0.269 (2.61%)	0.426 (4.13%)	0.594 (5.76%)	0.503 (4.88%)	**0.779 (7.56%)**
2 × 2 images	0.503 (4.88%)	0.660 (6.40%)	1.416 (13.7%)	0.829 (8.05%)	**1.641 (15.9%)**
2 × 3 images	0.389 (3.77%)	0.621 (6.03%)	1.068 (10.3%)	0.733 (7.11%)	**1.295 (12.5%)**
2 × 5 images	0.295 (2.86%)	0.509 (4.94%)	0.770 (7.47%)	0.589 (5.71%)	**0.969 (9.40%)**
2 × 7 images	0.281 (2.72%)	0.469 (4.55%)	0.712 (6.91%)	0.546 (5.30%)	**0.897 (8.71%)**

7. Conclusion

This work has shown that the ODP Optical Flow technique is very efficient for the recovery, by Particle Image Velocimetry in a planar section, of two or three velocity components of three-dimensional flows. The ODP-PIV system has been evaluated using the VSJ standard images and an associated standard protocol. The RMS error is within the 2-3% range for the two-component recovery and within the 4-8% range for the three-component recovery (on the STD01 to STD08, STD301, STD302, STD331 and STD337 Standard Images). Using more than two consecutive images always improve the accuracy and often significantly. Using the VSJ Custom-Made Standard Image generator program, the optimal image charactistics for the method have also been determined. One limitation of the ODP technique is that it is slow, especially when more than two consecutive images are used.

Comparison with other systems cannot be achievd yet since the ODP-PIV systems is currently the only one having been tested with the standard protocol on the VSJ test sequences. However, it has been observed, using another test set and test protocol that it performed much better than classical correlation using 32×32 and 48×48 interrogation windows (Quénot et al., 1998).

The PIV-STD synthetic images are very clean (without any noise) and, in this regard, may not be as representative of real data as it would be desirable. Though they are useful for comparing, on a quantitative and objective ground, the relative performances of PIV systems and for providing an estimation of their absolute performances, results might change significantly with real and noisy data. Therefore, experiments should also be conducted using real PIV data. The ODP-PIV has been proven to be very robust to noise using other synthetic data with noise and real data (Quénot et al., 1998), also publicly available for comparative performance evaluation from the LIMSI web site at: ftp://ftp.limsi.fr/~pub/quenot/opflow/testdata/piv/. Future work will consider the effects of both approximate camera calibration and noise for the performance evaluation of the ODP-PIV method and other methods using both synthetic and real data. The systematic error (currently unknown) of the ODP-PIV method sould also be investigated and characterized.

Acknowledgments

The author would like to thank Pr. Okamoto for his support for understanding and using the Standard Image test sequence, for building and maintaining the web site of the PIV-STD project, and for his advices in setting up the test protocol. The author also would like to thank Pr. Pakleza and Pr. Kowalewski for their help and advices for applying the ODP optical flow technique to the PIV problem.

References

Hesselink, L., Digital Image Processing in Flow Visualization, Annual Review in Fluid Mechanics, 20 (1988), 421-485.

Hu, H., Saga, T., Kobayashi, T., Okamoto, K. and Taniguchi, N., Evaluation of the Cross Correlation Method by Using PIV Standard Images, Journal of Visualization, 1 (1998), 87-94.

Huang, H. T., Fiedler, H. E. and Wang, J. J., Limitation and Improvement of PIV. part II: Particle Image Distortion, a Novel Technique,

Experiments in Fluids, 15 (1993), 263-273.
Merzkirch, W. and Gui, L. C., A method of Tracking Ensembles of Particle Images, Experiments in Fluids, 21 (1996), 465-468.
Okamoto, K., Nishio, S., Kobayashi, T. and Saga, T., Standard Images for Particle Image Velocimetry, Proceedings of the Second International Workshop on PIV1997 (Fukui), 229-236.
Quénot, G. M., The "Orthogonal Algorithm" for Optical Flow Detection Using Dynamic Programming, Proceedings of the International Conference on Acoustics, Speech and Signal Processing 1992 (San Francisco), 249-252.
Quénot, G. M., Computation of Optical Flow Using Dynamic Programming, Proceedings of the IAPR Workshop on Machine Vision Applications 1996 (Tokyo), 249-252.
Quénot, G. M., Pakleza, J. and Kowalewski, T. A., Particle Image Velocimetry with Optical Flow, Experiments in Fluids, 25-3 (1998), 177-189.
Quénot, G. M., Performance Evaluation of an Optical Flow for Particle Image Velocimetry, Proceedings of the Euromech Colloquium on Image Processing in Applied Mechanics, 1999 (Warsaw), 177-180.
Quénot, G. M. and Okamoto, K., A Standard Protocol for Quantitative Performance Evaluation of PIV systems, Proceedings of the 9th International Symposium on Flow Visualization, 2000 (Edinburgh).
Tokumaru, P. T. and Dimotakis, P. E., Image Correlation Velocimetry, Experiments in Fluids, 19 (1995), 1-15.
Willert, C. E. and Gharib, M., Digital Particle Image Velocimetry, Experiments in Fluids, 10 (1991), 181-193.

Author Profile

Georges M. Quénot : He received the engineer diploma from the French Polytechnic School in 1983, the M.S. degree in computer science from Grenoble University, France, in 1984, and the Ph.D. degree in computer science from Orsay, Paris XI University, France, in 1988. He has worked on computer architecture and VLSI circuit design for speech recognition and image processing. He is now a Researcher at the CLIPS-IMAG Laboratory of the Grenoble Joseph Fourier University where he is in charge of the image and video activities in the Multimedia Information Retrieval and Indexing group. He works on motion analysis techniques and their application to various domains, including Particle Image Velocimetry.